Coherent Fourier transform electrical pulse shaping

Shijun Xiao and Andrew M. Weiner

School of Electrical and Computer Engineering, Purdue University
West Lafayette, IN 47907-2035, U.S.A.
sxiao@ecn.purdue.edu ; amw@ecn.purdue.edu

Abstract: Fourier synthesis pulse shaping methods allowing generation of programmable, user defined femtosecond optical waveforms have been widely applied in ultrafast optical science and technology. In the electrical domain, arbitrary waveform generation is well established at frequencies below approximately 1 GHz, but is difficult at higher frequencies due to limitations in digital-to-analog converter technology. In this paper we demonstrate a method for electrical waveform synthesis at substantially higher frequencies (approximately 20 GHz electrical bandwidth) by combining Fourier optical pulse shaping (extended to hyperfine frequency resolution) and heterodyne optical to electrical conversion. Our scheme relies on coherent manipulation of fields and phases at all stages, both for processing in the optical domain and for conversion from the optical to the electrical domain. We illustrate this technique through a number of examples, including programmable retardation or advancement of short electrical pulses in time over a range exceeding ten pulse durations. Such optically implemented, coherent Fourier transform electrical pulse shaping should open new prospects in ultrawideband electromagnetics.

OCIS codes: (320.5540) Pulse shaping; (070.6020) Signal Processing; (350.4010) Microwaves.

References and links

1. A. M. Weiner, "Femtosecond pulse shaping using spatial light modulators," Rev. Sci. Instrum. **71**, 1929-1960 (2000).
2. J. D. McKinney, D. E. Leaird, A. M. Weiner, "Millimeter-wave arbitrary waveform generation with a direct space-to-time pulse shaper," Opt. Lett. **27**, 1345-1347 (2002).
3. I. S. Lin, J. D. McKinney, and A. M. Weiner, "Photonic Synthesis of Broadband Microwave Arbitrary Waveforms Applicable to Ultra-Wideband Communication," IEEE Microwave Wireless Component Lett. **15**, 226-228 (2005).
4. J. Chou, Y. Han, and B. Jalai, "Adaptive rf-photonic arbitrary waveform generator," IEEE Photon. Tech. Lett., **15**, 581-583 (2003).
5. Y. Liu, S. Park, and A. M. Weiner, "Enhancement of narrow-band terahertz radiation from photoconducting antennas by optical pulse shaping," Opt. Lett. **21**, 1762 (1996).
6. J. H. Reed, Ed., *An Introduction to Ultra Wideband Communication Systems* (Prentice Hall, 2005).
7. R. J. Fontana, "Recent system applications of short-pulse ultra-wideband (UWB) technology," invited, IEEE Trans. Microwave Theory Technol. **52**, 2087-2104 (2004).
8. H. L. Bertoni, L. Carin, L. B. Felsen, *Ultra-wideband, short-pulse electromagnetics* (New York : Plenum Press, 1993).
9. A. Vilcot, B. Cabon, and J. Chazelas, *Microwave Photonics: from components to applications and systems* (Boston: Kluwer Academic, 2003).
10. J. Capmany, B. Ortega, D. Pastor and S. Sales, "Discrete-Time Optical Processing of Microwave Signals," invited, IEEE/OSA J. Lightwave Technol. **23**, 702-723 (2005).
11. S. Xiao and A. M. Weiner, "Coherent photonic processing of microwave signals using spatial light modulator: programmable amplitude filters," IEEE/OSA J. Lightwave Technol. Special Issue of Optical Signal Processing (to be published).

#67525 - $15.00 USD Received 27 January 2006; revised 20 March 2006; accepted 23 March 2006

12. M. Shirasaki, "Large angular dispersion by a virtually imaged phased array and its application to a wavelength demultiplexer," Opt. Lett. **21**, 366-368 (1996).
13. S. Xiao and A. M. Weiner, "An Eight-Channel Hyperfine Wavelength Demultiplexer Using a Virtually-Imaged Phased-Array (VIPA)," IEEE Photonics Technol. Lett. **17**, 372-374 (2005).
14. J. P. Heritage, A. M. Weiner and R. N. Thurston, "Picosecond pulse shaping by spectral phase and amplitude manipulation," Opt. Lett. **10**, 609-611 (1985)
15. W. Ng, A. A. Walston, G. L. Tangonan, J. J. Lee, I. L. Newberg, and N. Bernsterin, "The first demonstration of an optically steered microwave phased array antenna using true-time-delay" IEEE J. Lightwave Technol., **9**, 1124-1131 (1991).
16. B. Ortega, J. L. Cruz, J. Capmany, M. V. Andres, and D. Pastor, "Variable delay line for phased-antenna based on a chirped fiber grating," IEEE Trans. Microwave Theory Technol., **48**, 1352-1360 (2000).
17. J. Yang, S. Tjin and N. Ngao, "All chirped fiber gratings based true-time delay for phased-array antenna beam forming," Appl. Phys. B **80**, 703-706 (2005).
18. S. Xiao, A. M. Weiner and C. Lin, "A dispersion law for virtually-imaged phased array based on paraxial wave theory," IEEE J. Quantum Electron. **40**, 420 (2004)
19. Y. Vlasov, M. O'Boyle, H. Hamann and S. McNab, "Active control of slow light on a chip with photonic crystal waveguides," Nature **438**, 65 (2005)
20. M. Bigelow, N. Lepeshkin and R. Boyd, "Superluminal and slow light propagation in a room-temperature solid," Science **301**, 200 (2003)
21. L. J. Wang, A. Kuzmich and A. Dogariu, "Gain-assisted superluminal light propagation," Nature **406**, 277 (2000)

1. Introduction

The ability to generate and manipulate complex electromagnetic signals has pervasive impact in science and technology. For example, cellular radio uses families of pseudonoise waveforms to enable multiple-access radio communications with minimal interference between simultaneous users, and sophisticated pulse sequences are exploited for high quality magnetic resonance imaging. In the electrical domain, instruments termed arbitrary waveform generators (AWGs) provide the ability to realize user specified waveforms for applications such as design, simulation, and test of communications systems, radar, semiconductor logic, and sensors. However, due to limitations in digital-to-analog converter technology, electrical AWGs are limited to bandwidths below approximately 2 GHz. In the optical domain, on the other hand, pulse shaping techniques, in which phase and amplitude manipulation of optical spectral components allow synthesis of user-specified ultrashort (femtosecond) pulse fields according to a Fourier transform relationship, have been developed and widely adopted [1]. Applications are diverse, including coherent control of chemical reactions, molecular motions, and quantum mechanical wave packets, single cycle pulse generation approaching the attosecond regime, frequency selective nonlinear microscopy and imaging, transmission of femtosecond pulses over optical fiber links, and lightwave communications schemes based on phase-coded ultrashort pulse waveforms. In most applications of such optical AWG, the coherence of the optical field is of key importance – i.e., optical phase is intentionally manipulated and exploited. Because of the success of optical pulse shaping at very fast time scales, it is natural to ask whether such optical technology can be exploited to extend electrical AWG to higher frequencies. Indeed, a few groups have reported experiments in which shaped optical waveforms impinge on an optical-to-electrical (O/E) converter, whereby the shaped optical waveform is transduced into a shaped electrical waveform burst, with electrical frequencies ranging from GHz to THz depending on experimental parameters [2-5]. However, these experiments depend only on manipulation of optical intensity, as O/Es convert optical intensity directly into electrical current. Thus, optical phase is not exploited (although manipulation of electrical phase is possible nevertheless). In this paper we report a new method for electrical AWG based on optical pulse shaping. Unlike previous work our method relies on coherent manipulation of phase at all stages, both for processing in the optical domain and for conversion from the optical to the electrical domain. We also demonstrate how to tune our experiment from the

#67525 - $15.00 USD Received 27 January 2006; revised 20 March 2006; accepted 23 March 2006

coherent regime (optical field based) to the incoherent regime (optical intensity based). The present experiments may be considered as the first close electrical analogue to the Fourier transform waveform synthesis approach widely used in ultrafast optics.

In this paper for the first time we demonstrate our photonic processing concept by reprogrammably reshaping pulsed electrical waveforms with temporal features well below 100 ps and frequency content in the range DC to ~ 20 GHz via parallel photonic manipulation of the Fourier phases. Our results are well beyond the capability of conventional electrical AWG technology and are of close relevance for ultra-wideband (UWB) electromagnetics [6-8], a field involving generation and reception of short-pulse wireless waveforms with very large fractional bandwidths [8] that has received intense attention in recent years. UWB applications include wireless communications (3.1-10.6 GHz band, as per FCC regulation), collision avoidance radar (22-29 GHz band), and ground-penetrating radar. The very large bandwidths of UWB signals allow significant waveform energy at low power spectral density, thereby permitting overlay with conventional narrow-band radio-frequency applications. Furthermore, for UWB radar and positioning systems, extremely broad bandwidths map onto high temporal and spatial resolution (down to millimeters). Current UWB applications generally utilize relatively simple waveforms (pulses), with limited capability for waveform control. Our work allowing essentially arbitrary waveform reshaping under computer control opens the possibility of new classes of UWB systems, for example, systems that exploit families of phase-coded waveforms specially designed for enhanced multiple-access capabilities. Examples demonstrated in this paper include programmable reshaping of unipolar (half-cycle) electrical pulses into single-cycle (bipolar) waveforms and programmable advancement or retardation in time of short electrical pulses over a range exceeding ten pulse durations.

It is important to note that photonic processing of microwave signals [9-11] has been the subject of substantial research effort dating back nearly thirty years. Compared to purely electronic implementations, photonics offers substantial advantages in the areas of wide operating bandwidth, reconfigurability, and immunity to electromagnetic interference. Generally, the input microwave signal is used to drive an electro-optic modulator, which imposes the microwave signal onto an optical carrier wave. The resulting optical signal is manipulated as desired via photonic techniques and then directed to an O/E converter to get back to the microwave domain. In the previous large body of work [9, 10], photonic processing was achieved in a tapped delay line (time domain) architecture, in which delayed samples of the optical power are incoherently combined. This has led to a number of demonstrations of microwave amplitude filters difficult to realize via electronics alone. However, to our knowledge, none of this previous work has addressed synthesis of broadband microwave phase filters. In contrast to previous work, our experiments achieve photonic processing via parallel and fully coherent manipulation of the field in the optical frequency domain. This architecture provides direct access to spectral phase, allowing synthesis of essentially arbitrary microwave phase filters over ultrawide bandwidth, for the first time to our knowledge. In contrast to traditional narrowband radio-frequency and wireless systems, phase effects and their control are of tremendous importance over ultrawide electrical bands. For example, common antennas optimized for broadband transmission bandwidth are in most cases not optimized for good phase response, which leads to strong distortions in ultrawideband pulsed operation [6, 7]. The ability to manipulate spectral phase would enable compensation of such distortions, much as optical dispersion compensation technologies are commonly employed to mitigate pulse broadening and distortion in optical fiber communications.

2. Experimental setups

Figure 1(a) shows our schematic experimental setup. A continuous-wave laser provides an optical carrier at 1.55 μm wavelength (linewidth ~0.1 pm or 12.5 MHz). The optical carrier is

#67525 - $15.00 USD Received 27 January 2006; revised 20 March 2006; accepted 23 March 2006

sent into an integrated Mach-Zehnder electro-optic modulator (30 GHz electrical modulation bandwidth) driven by a pulsed UWB electrical signal (~30 ps duration full-width at half-maximum, zero frequency to ~20 GHz electrical bandwidth). The pulsed drive signal has a peak voltage of ~200 mV, intentionally kept well below the voltage (V_π = 5V) required to drive the modulator output to zero. This results in a linear modulation response, such that the Fourier spectrum of the electrical driving pulse is transferred directly into the optical domain. The resulting optical spectrum is normally centered about a narrowband carrier, representing the portion of the input optical field that is not modulated (Fig. 1(b)). The intensity of the narrowband carrier compared to the broadband pulse-modulated spectrum can be controlled through a bias voltage V_b applied to the modulator. We have run experiments with $V_b = V_\pi/2$, in which case the carrier intensity exceeds that of the modulated optical signal component, and with $V_b = V_\pi$, in which case the carrier is completely suppressed (Fig. 1(c)). In either case the output signal from the modulator is processed by a hyperfine Fourier transform pulse shaper (discussed below), which imposes the desired phase vs. frequency characteristic onto the optical spectrum. The optical signal after the hyperfine pulse shaper is directed onto a fast photodiode (60 GHz electrical bandwidth), which functions as the O/E converter, and the resulting electrical waveform is measured (after a DC blocking filter in the case of coherent heterodyne detection) on a sampling oscilloscope with 50 GHz electrical bandwidth. Optical amplifiers (not shown) are used to adjust the power level incident onto the photodiode. The output waveform my be understood on the basis of the following simple equation

$$i(t) \propto I(t) \propto A^2 + |u(t)|^2 + 2A\,\mathrm{Re}\{u(t)\} \qquad (1)$$

where i(t) is the photodiode current, assumed to be linear in the optical intensity I(t) averaged over the oscillations of the optical carrier frequency, *A* is the carrier amplitude (assumed without loss of generality to be real), and Re{-} is the real part. *u(t)* corresponds to the inverse Fourier transform of the (complex) optical spectral amplitude function, excluding carrier, which would give the complex pulse amplitude in time in pure optical pulse shaping. When a strong carrier wave is present (*A* much larger than the peak of *u*), heterodyne beating arising from the coherent interference between carrier and modulated optical field components dominates – i.e., the dominant time-dependent term is proportional to *Re{u(t)}*. In this case optical phase information is retained and transferred coherently into the electrical domain (Fig. 1(b)). On the other hand, since photodiodes convert directly from optical power to electrical current, direct detection (which occurs when the carrier is suppressed, *A=0*, Fig. 1(c)) yields unipolar electrical waveforms $|u(t)|^2$. Optical phase information is lost in this incoherent transformation process.

#67525 - $15.00 USD Received 27 January 2006; revised 20 March 2006; accepted 23 March 2006

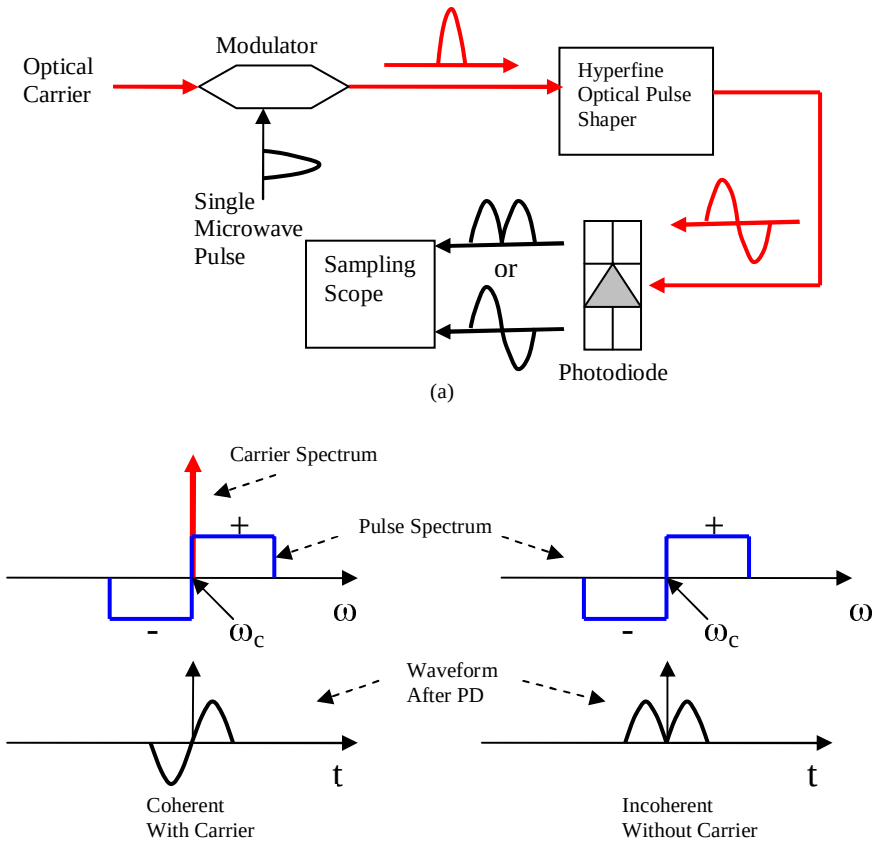

Fig. 1. (a) Schematic layout for photonic spectral phase shaping of ultrawideband microwave pulses. The red color indicates optical fields, and the black color indicates microwave electrical signals. Electrical outputs are sketched under both incoherent and coherent optical-to-electrical conversion. (b,c) Sketches illustrating coherent (b) and incoherent (c) operation. The upper line shows the frequency-dependent optical field corresponding to a specific setting (refer to discussion in connection with Fig. 3) of the hyperfine optical pulse shaper, either with (b) or without (c) a superimposed optical carrier. The lower line sketches the resulting time-dependent voltage amplitudes after conversion into the electrical domain.

Figure 2 shows the setup of our fiber-coupled, hyperfine optical pulse shaper. The setup is similar to that used extensively for femtosecond pulse shaping [1], except that the diffraction grating normally used as a spectral disperser is replaced by a virtually-imaged phased-array device [12] (or VIPA). Briefly, different optical frequency components are dispersed to different output angles by the VIPA and then focused to different spatial positions at the back focal plane of the lens. A programmable liquid crystal spatial light modulator (SLM) is placed at this back focal plane. The SLM consists two aligned layers, and each layer consists of 128 pixels, arranged along a line on 100 μm centers. Each pixel can be programmed for simultaneous and independent control of transmitted optical intensity and of optical phase. A flat mirror very placed close to the SLM reflects the light for a double pass through the setup. Further details are given in the caption to Fig. 2. After the optical frequencies are recombined in the second pass through the VIPA, the output signal is extracted using an optical circulator. In the case of a short pulse optical input, the output waveform in time is determined by the inverse Fourier transform of the complex spatial pattern transferred from the SLM onto the optical spectrum.

#67525 - $15.00 USD Received 27 January 2006; revised 20 March 2006; accepted 23 March 2006

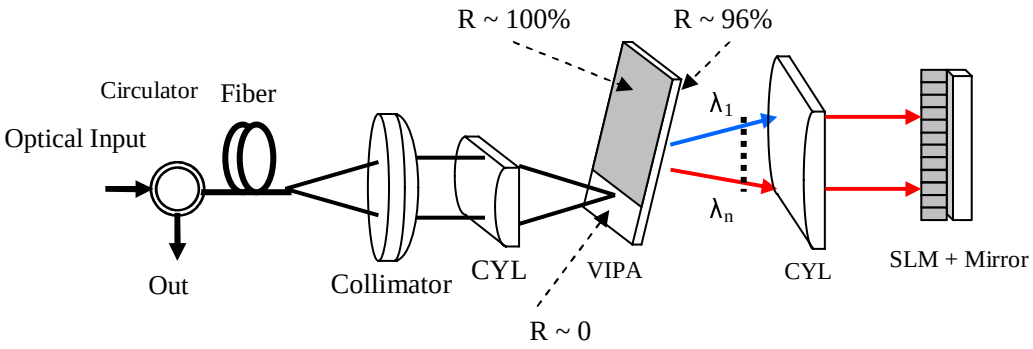

Fig. 2. Setup of (optical) hyperfine Fourier transform pulse shaper based on a virtually-imaged phased array (VIPA). CYL: cylindrical lens (300 mm focal length). SLM: spatial light modulator. R: optical power reflectivity. The VIPA consists of a 1.5 mm thick glass etalon with an anti-reflection coated entrance window, front and back reflectivities of approximately 100% and 96%, respectively, and a free spectral range of 50 GHz. The incident angle onto the VIPA is ~ 2.5 deg. The optical insertion loss from the input to output of the circulator is ~ 13 dB in our setup. The two-layered SLM is programmed to control the optical phase for frequencies falling between pixels #40 and #80 (a 28 GHz frequency band) and to block frequencies falling outside this range. The optical carrier is centered at pixel #60. The spectral dispersion amounts to 600-700 MHz per pixel, with lower optical frequencies at higher pixel numbers. A filter programmed for a one-pixel wide passband (not shown) yields a -3dB bandwidth of 500-625 MHz, demonstrating that each pixel controls an independent band of frequencies.

It is important briefly to discuss the VIPA device. As shown in Fig. 2, the VIPA is similar to the common optical etalon structure, with the difference that light is injected at an angle through an anti-reflection coated window. After injection into the VIPA, the light is trapped between two reflecting surfaces and bounces back and forth. This gives rise to multiple-beam interference effects that result in spectral (angular) dispersion, and the diffraction efficiency is relatively high and can be comparable to diffraction gratings. Mechanisms that limit diffraction efficiency include diffraction into multiple orders and clipping of the tails of the input beam as it is injected into the VIPA [13]. An important advantage of the VIPA is that its spectral dispersion can be much larger compared to gratings, which results in proportionally enhanced spectral resolution. We have recently performed a series of studies investigating VIPAs for applications in optical demultiplexing and optical signal processing. Our results [11, 13] demonstrate hyperfine optical filters with linewidths in the 600 MHz range. Here, incorporating such performance into a programmable pulse shaper geometry, we are now able to obtain parallel and essentially arbitrary control over optical phase and amplitude (here we focus on phase) over a 28 GHz frequency band with ~600 MHz resolution. This very high spectral resolution, between one and two orders of magnitude finer than typically obtained with grating-based pulse shapers, is an essential enabler for the current work, since the overall bandwidth of interest – while large by electrical standards – is orders of magnitude narrower than usually considered in femtosecond optics applications.

3. Experimental results

Figure 3 shows a first set of experimental results demonstrating UWB waveform synthesis. Here half of the optical spectrum is programmed for 0 phase and half for π phase. This means that optical field is antisymmetric in frequency – the field amplitude changes sign at the center of the spectrum, as sketched in Figs. 1(b-c). According to the inverse Fourier transform, the resulting waveform in the time domain is a pulse doublet, with a phase reversal between the pulses; i.e., the field is an odd function of time [14]. Figure 3(a) shows the UWB electrical waveform generated after O/E conversion, in the strong carrier wave case ($V_b = V_\pi/2$). As

#67525 - $15.00 USD Received 27 January 2006; revised 20 March 2006; accepted 23 March 2006

sketched in Fig. 1(b), the electrical waveform is an "odd" pulse – a bipolar, odd function of time – corresponding to a single electrical cycle at ~ 10 GHz. A similar experiment is performed for Fig. 3(b), except that the SLM is programmed such that the 0 phase and π phase portions of the optical spectrum are interchanged. This is expected to change the polarity both of the spectrum and of the resulting time domain waveform compared to Fig. 1(b). The data in Fig. 3(b) confirm this expectation – a single electrical cycle is again generated, but now with initial positive voltage, in contrast to the initial negative voltage in Fig. 3(a). These data clearly confirm the ability to transduce shaped optical pulses coherently into shaped electrical waveforms. Figure 3(c) shows data for the same optical filter function as in Fig. 3(a), but now in the case of strong carrier suppression ($V_b = V_\pi$). In this regime the square law nature of the photodiode yields an electrical output proportional to the time-dependent optical power. This results in a unipolar electrical output – still a pulse doublet, but now an even function of time with no phase reversal. These data clearly demonstrate the ability to tune our experiments from the coherent regime (optical field based) to the incoherent regime (optical intensity based).

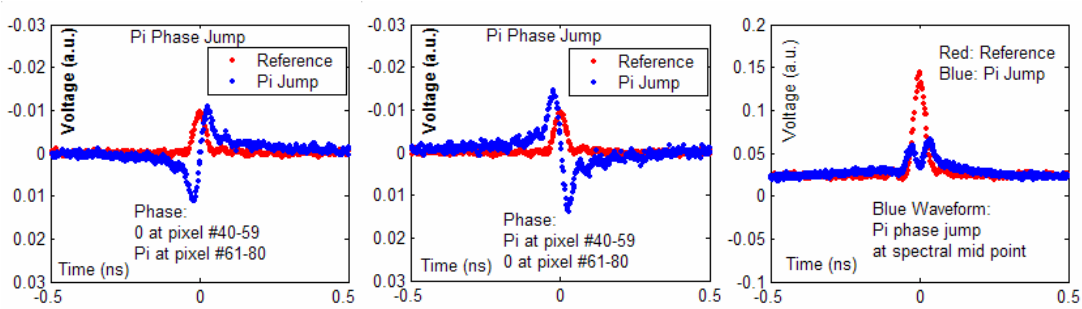

(a) (b) (c)

Fig. 3. Electrical doublet pulses generated via insertion of a π phase jump onto the optical spectrum (see sketches in Fig. 1). Electrical reference pulse measured without phase shaping is shown in red; shaped waveforms shown in blue. (a) - (b) are coherent optical-to-electrical conversion in presence of strong carrier wave. The unipolar (~half-cycle) electrical input pulse is converted into a bipolar (~ single-cycle) electrical output. The polarity of the electrical output is switched by interchanging the SLM pixels programmed for 0 and π phase shifts, respectively. Here a wideband electrical DC blocking filter is used to suppress the constant background due to the carrier power. (c) is incoherent optical-to-electrical conversion with suppressed carrier. The input pulse is converted into a unipolar pulse doublet.

#67525 - $15.00 USD Received 27 January 2006; revised 20 March 2006; accepted 23 March 2006

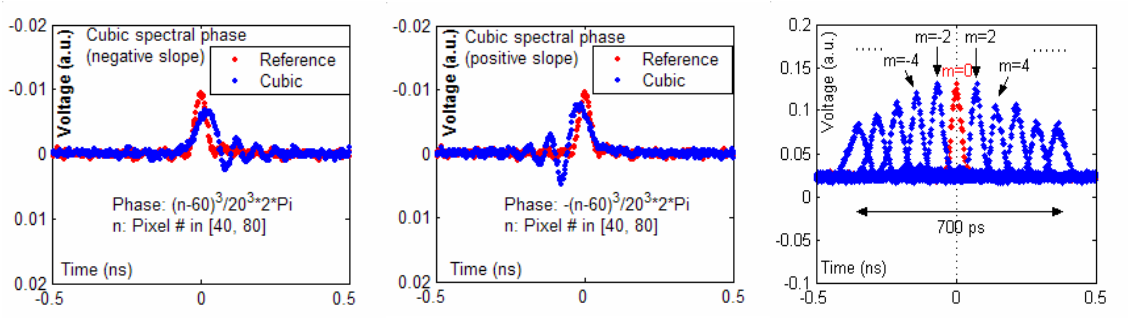

(a) (b) (c)

Fig. 4. (a)-(b) Ultrafast, ultrawideband electrical pulse shaping via cubic spectral phase and coherent detection. Both (a) and (b) show an asymmetric pulse distortion with a damped ringing tail, as expected. However, the signs of the cubic spectral phase are opposite, leading to a reversal in the sense of the asymmetry with respect to time. (c) Ultrafast, ultrawideband electrical true-time-delay via linear spectral phase shaping. Both retardation or advancement in time is possible, depending on the sign of the linear spectral phase. The case *m=0*, for which the SLM is essentially deactivated, is taken as the time reference (plotted in red). Data are shown for incoherent detection, although in this case essentially identical results are obtained in the coherent detection case.

As a second example of UWB waveform synthesis, we use the hyperfine pulse shaper to generate a cubic spectral phase function. Specifically, the SLM is programmed for a phase profile $\psi(n) = \pm 2\pi\left[(n-60)/20\right]^3$ for pixel numbers (n) in the range [40, 80]. It is well known in ultrafast science that cubic spectral phase leads to an asymmetric waveform with an oscillatory tail appearing on one side of the main pulse (which side depends on the sign of the cubic phase). This effect may be understood through the well known relation

$$\tau(\omega) = \frac{-\partial\psi(\omega)}{\partial\omega} \tag{2}$$

which relates the dispersion, i.e., the frequency-dependent group delay function $\tau(\omega)$, to the derivative of frequency-dependent phase with respect to angular frequency ω. For the cubic phase case, $\tau(\omega)$ is quadratic, which means that the dispersion broadens the pulse asymmetrically towards either positive time or negative time, again depending on the sign of cubic phase. Furthermore, the quadratic dispersion function imparts the same time shift to low and high frequency components as long as they are offset equally from the center frequency, these frequencies can interfere to yield a ringing in time. Data are shown in Figs. 4(a)-(b) for the two signs of cubic phase, both in the strong carrier wave (fully coherent) regime. The observed asymmetric distortions closely resemble the analogous waveform distortions known in ultrafast optics, and as expected the change in the sign of phase reverses the sense of the time axis relative to the waveform asymmetry. An important point is that the data of Fig. 4 are in the electrical domain. In contrast to the field of ultrafast optics, synthesis of ultrawideband electrical waveforms via programmable manipulation of spectral phase has not previously been reported.

As a final example, we consider programmable control of time delay. Referring to Eq. (2), we observe that a frequency-independent time delay corresponds to a phase function $\psi(\omega)$ that is linear in frequency. Accordingly, in our experiments the output signal can be shifted forward or backward in time by programming the SLM for appropriate linear phase functions. From the applications perspective, techniques for achieving such true-time-delays are of extensive interest for wide instantaneous bandwidth beam steering of phased array antenna systems [15-17]. Figure 4(c) shows our experimental results. Data are shown for eleven different cases, where the SLM is programmed for a phase profile

#67525 - $15.00 USD Received 27 January 2006; revised 20 March 2006; accepted 23 March 2006

$\psi(n) = \frac{m\pi(n-60)}{20}$, for $m = -10, -8 \ldots 0 \ldots 8, 10$ and pixel numbers (n) in the range [40, 80]. The data shown are for the case of incoherent operation, although essentially identical results are obtained under coherent operation. The case *m=0*, for which the SLM is essentially deactivated, is taken as the time reference (*t=0* in plot); in this way fixed delays associated with propagation through the hyperfine pulse shaper and optical and electrical cables are taken out. Each of the traces is shifted to distinct time positions, either forward or backward in time depending on the sign of *m*. From Eq. (2), we expect a time shift between adjacent pulses of $(2\pi/20)/(2\pi*0.7GHz) \approx 71$ *ps*, and total time delay of 710 ps. This is in excellent agreement with the experimental results, which demonstrate 700 ps total time delay, approximately 15 times the duration of the individual pulse widths (45 ps for the *m=0* pulse), with minimal distortion. The small pulse broadening observed for the larger time shifts is attributed to curvature in the VIPA's spectral dispersion function [18], i.e, in the mapping of optical frequency to spatial location, which is not taken into account in programming the SLM in this experiment.

In the optical domain, manipulation of time delay has been the subject of considerable recent interest through studies of slow as well as fast (superluminal) light [19-21], both for fundamental reasons and due to potential for new classes of devices (e.g., optical buffers). In these studies the group velocity of light is modified by a strong frequency variation in refractive index in the vicinity either of a photonic crystal band edge [19] or of narrow absorption or gain resonances [20-21]. In contrast, the programmable increases or decreases in propagation time in our experiments (either in the optical or in the electrical domain) rely on a more general principle: direct parallel manipulation of frequency-dependent optical phase through Eq. (2). Experiments on the control of time delay via spectral phase pulse shaping have been performed previously within the context of ultrafast optics [1]. Comparing again to slow/fast light experiments [19-21], the fractional change in group velocity in our experiments is relatively small, roughly ±10% relative to the 4 ns free-space propagation delay within the pulse shaper apparatus. On the other hand, the ability to displace the pulse over a time range exceeding its duration by more than an order of magnitude, with little distortion, is far superior to results reported in slow/fast light experiments, where strong frequency-dependent loss or group velocity dispersion associated with resonant structures has usually limited operation to time delays on the order of the pulse duration or less.

4. Conclusion

In summary, we have demonstrated how Fourier transform pulse shaping techniques, developed and widely applied in the field of ultrafast optics, can be extended for ultrawideband electrical waveform shaping. This photonic approach to electrical arbitrary waveform generation provides bandwidths substantially beyond what is possible using electronic technologies. For the first time our work realizes coherent manipulation of phase at all stages, both for processing in the optical domain and for subsequent optical to electrical conversion. We also show how to tune between coherent and incoherent processing. From the applications perspective, our work offers new possibilities for transmission of ultrashort electrical signals over antenna systems and for new classes of ultrawideband wireless systems based on transmission and coherent processing of phase-modulated electrical transients. From a fundamental perspective, we have demonstrated programmable retardation or advancement of electrical group delay via spectral phase shaping and contrasted this method with recent slow/fast light approaches.

For further development of this technology, it is desirable to build an electrical pulse shaper with high update speed and large temporal aperture. Liquid crystal SLMs, used in the current work, support updates in tens of milliseconds, possible extendable down to a few milliseconds. For higher update speeds down to approximately microseconds, MEMs arrays

#67525 - $15.00 USD Received 27 January 2006; revised 20 March 2006; accepted 23 March 2006

may be a good option. Larger temporal aperture requires higher spectral resolution from the optical pulse shaper. The spectral resolution of our VIPA shaper can be further improved by decreasing its FSR. On the other hand, reducing the FSR limits the bandwidth of the shaper, which affects the temporal resolution; this illustrates the trade-off between temporal aperture and temporal resolution. Because of this trade-off, time-bandwidth product is a good way to describe the complexity of the generated electrical waveforms. For our current case, the shaper has a FSR of 50 GHz while the electrical pulse has a full bandwidth of 28 GHz. This means it should be possible to improve the time-bandwidth product by almost a factor of two without major changes.

We gratefully acknowledge Avanex Corporation for donation of the VIPA device.

#67525 - $15.00 USD Received 27 January 2006; revised 20 March 2006; accepted 23 March 2006